Siesmic Network Data From Quetta, Pakistan: The Chaman Fault and the Fault Related to the 30 May 1935 Earthquake[1]

J. ARMBRUSTER, L. SEEBER, R. QUITTMEYER & A. FARAH

Abstract: Preliminary results from a telemetered seismic network in the Quetta area indicate seismic activity along the Quetta fault that ruptured during the 30 May 1935 earthquake (M = 7.5) and along the Chaman fault. However, the seismicity is concentrated in sections of these faults contiguous to, but not included in, the latest major rupture of each fault.

The epicenter and the surface effects of the 1935 Quetta earthquake suggest that the associated rupture propagated northward from Kalat to Quetta where it was clearly associated with the Chiltan fault. A number of well-located, shallow (0-15 km deep) hypocenters fall within the section of this fault-zone just north of Quetta. A composite fault-plane solution indicates left-lateral strike slip for the Quetta fault.

The last known large rupture on the Chaman fault occurred on 20 December 1892 and it is recognized from about latitude 30.3° northward. No instrumental or felt earthquakes are reported for the section of the Chaman fault south of this latitude until 1975. Since then, the record of the Chaman fault consists of 3 of the 4 teleseismic epicenters (3 October 1975, M_s 6.7 and M 6.4; 16 May 1978, M_s 5.9) and most of the epicenters from the network data (June to November 1978) in a 2° square centered at Quetta. This increase in seismicity in the southern portion of the Chaman fault warrants careful consideration as a premonitory signal.

The Chaman fault-zone south of the 1892 break is a series of subparallel left-lateral strike-slip faults which include the Quetta fault. Seismicity in this section is high, but it does not include any major event (M > 7.5). A comparison between this section of the Chaman fault system and the San Andreas fault system south of the big bend is suggested.

INTRODUCTION

The city of Quetta is strategically located at the apex of the Sibi re-entrant that divides the north-south trending Kirthar-Brahui ranges from the Loralai (Quetta) transverse ranges (Figures 1 and 4). The Chaman fault is the most obvious surface expression of the continent-continent boundary of the Indian plate and the Afghanistan block of the Eurasian plate. This fault strikes NNE through the town of Chaman, 70 km WNW of Quetta. In the Spring of 1978 a network of five telemetered seismic stations was established in the Quetta area for the study of tectonics and earthquake prediction in a cooperative effort between the Lamont-Doherty Geological Observatory, New York, and the Geological Survey of Pakistan, Quetta. Because the system response of these seismic stations has very high displacement gains ($\sim 10^6$) at the high frequencies typical of local earthquakes, numerous small-magnitude earthquakes can be recorded and studied. The signals from these five stations are continuously transmitted to the offices of the Geological Survey of Pakistan in Quetta where they are recorded on a common time base.

The hypocenter and first-motion data from 62 local earthquakes obtained from the Quetta seismic network in a two month period in 1978 are here interpreted together with teleseismic and geologic data in a first attempt to decipher the pattern of ongoing activity in the tectonically complex Quetta region.

TECTONIC SETTING

According to the theory of plate tectonics, the Indian plate is moving northward with respect to its adjacent stable block, the Eurasian plate (Molnar and Tapponnier, 1975; Fig. 1, inset). The rate of convergence is approximately 3.5 cm/yr near the longitude of Quetta (Minster and Jordan, 1978; Fig. 8). The Chaman fault (Figure 1) is usually considered the active boundary between the Indian plate and the microplates of Iran and Afghanistan which may be only loosely attached to Eurasia (Powell, 1979). Plate tectonics requires left-lateral strike-slip on this boundary. This left-lateral motion may not be fully taken up by the Chaman fault, but it may occur on a number of subparallel faults within a wide zone of deformation.

[1] Lamont-Doherty, Geological Observatory Contribution No. 2804.

Proc. Intern. Commit. Geodynamics, Grp. 6, Mtg. Peshawar, Nov. 23-29, 1979: Spec. Issue, Geol. Bull. Univ. Peshawar, Vol. 13, 1980.

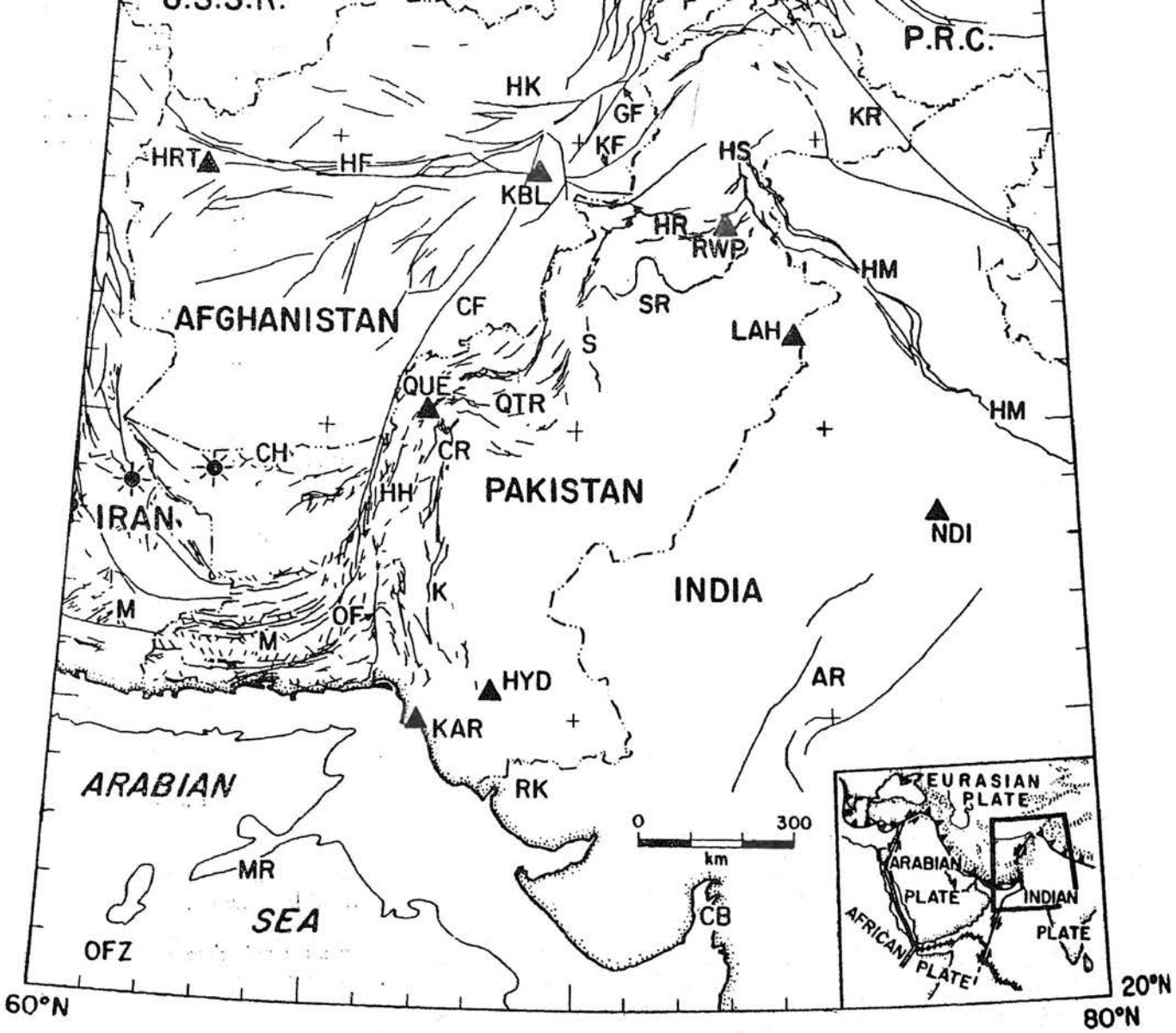

Fig. 1. Index map of the northwestern boundary of the Indian subcontinent (from Quittmeyer and Jacob, 1979). Mapped surface faults are shown. The 2 km sea-depth contour is also shown. The filled circles in Iran represent centers of Quaternary volcanism. Geographic features indicated are as follows: AR = Aravalli range, CB = Cambay basin, CF = Chaman fault, CH = Chagai hills, CR = Central Brahui range, GF = Gardez fault, HR = Hazara range, HF = Herat fault, HH = Harboi hills, HK = Hindu Kush region, HM = Himalayas, HS = Hazara-Kashmir syntaxis, K = Kirthar range proper, KF = Kunar fault, KR = Karakorum region, M = Makran region, OF = Ornach-Nal fault, OFZ = Owen fracture zone, P = Pamirs, QTR = Quetta transverse ranges, RK = Rann of Kutch, S = Sulaiman range and SR = Salt range. Several cities are indicated by filled triangles: HRT = Herat, HYD = Hyderabad, KAR = Karachi, KBL = Kabul, LAH = Lahore, NDI = New Delhi, QUE = Queta, RWP = Rawalpindi. The inset in the lower right hand corner shows the plate tectonic setting of the region.

Quetta lies within the Baluchistan geosyncline which is part of the Mesozoic and early Cenozoic Tethyan belt (Jones, 1961). A tectonic axis divides this broad depositional belt into two basins, a western basin with a western source area and an eastern basin with an eastern source area. Ultrabasic submarine volcanics interpreted as an ophiolitic suture-zone between the Indian plate and the microplates of Afghanistan occur along this axis. This suture or axial zone and other geologic structures bend at the apex of the Sibi-

re-entrant. The Tethys ocean closed here in the Oligocene, and the Oligocene-Pleistocene is represented in the Quetta area by marine deposits grading up into detridal molasse-like deposits which are the youngest rock formations in the area. Topographic lows are filled with recent alluvium.

The Quetta area has been the location of a number of large destructive earthquakes (Figures 2, 3, and 4). The general north-northeast trend of the elongated mezoseismal zones observed in 1892, 1931 and 1935 is consistent with the observed geologic structure and the direction of motion of India with respect to Eurasia. However, the transverse trend of the mezoseismal

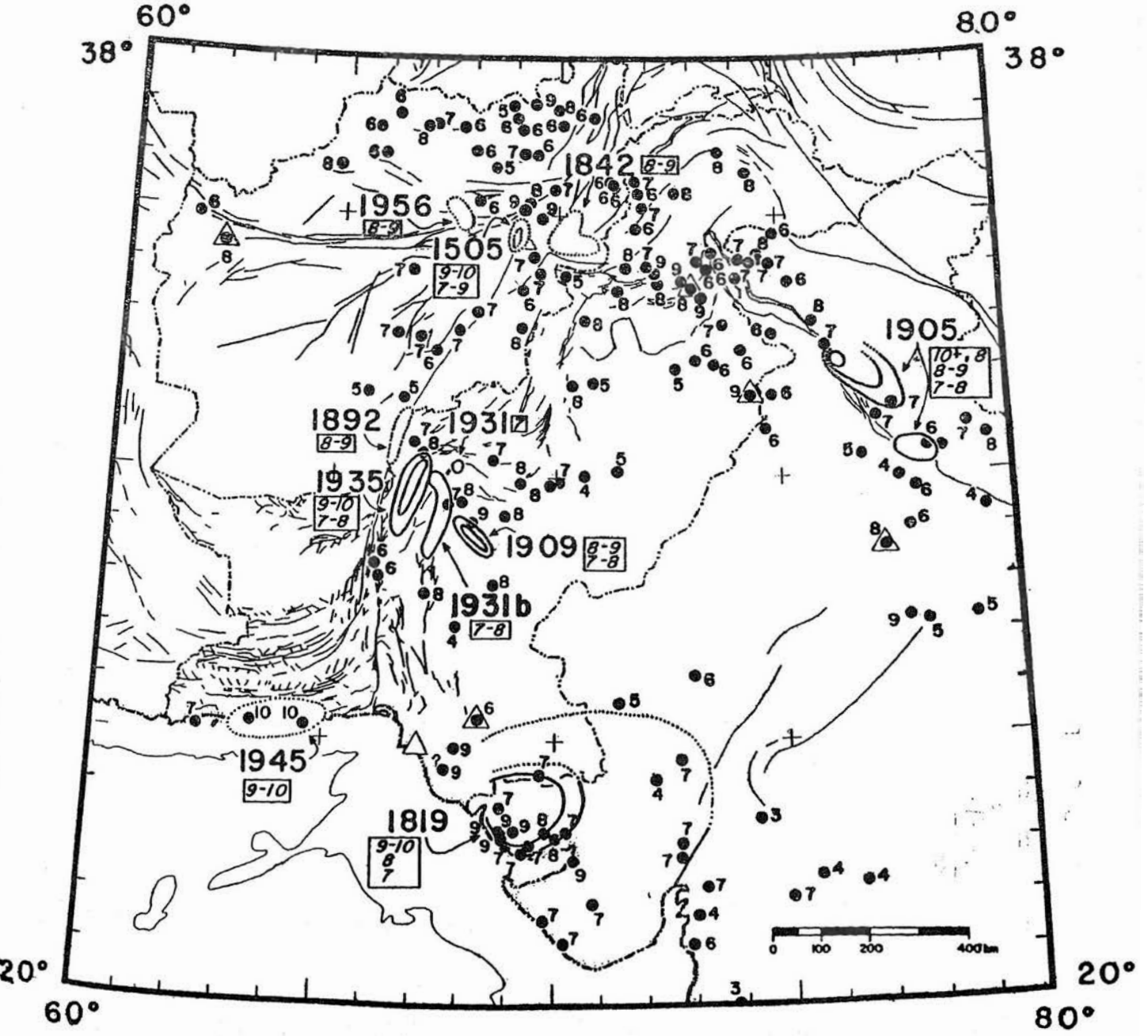

Fig. 2. Map of maximum documented intensity (Modified Mercalli Scale) at any given location (Quittmeyer *et al.*, 1979). Data for the time period ~ 25 A.D. to 1972 are shown. Isoseismal lines (dotted where inferred) are plotted for some of the larger events. The year of occurrence for each such large event is indicated. The intensity value associated with a given isoseismal line is indicated in the box near each data. The first value given is for the innermost isoseismal line, etc. Isoseismal lines for the 1905 event are after Middlemiss (1910), those for the 1909 event are after Heron (1911), and those for the 1931, 1931b, and 1935 events are after West (1934, 1935). The open triangles represent the same cities shown in Figure 1.

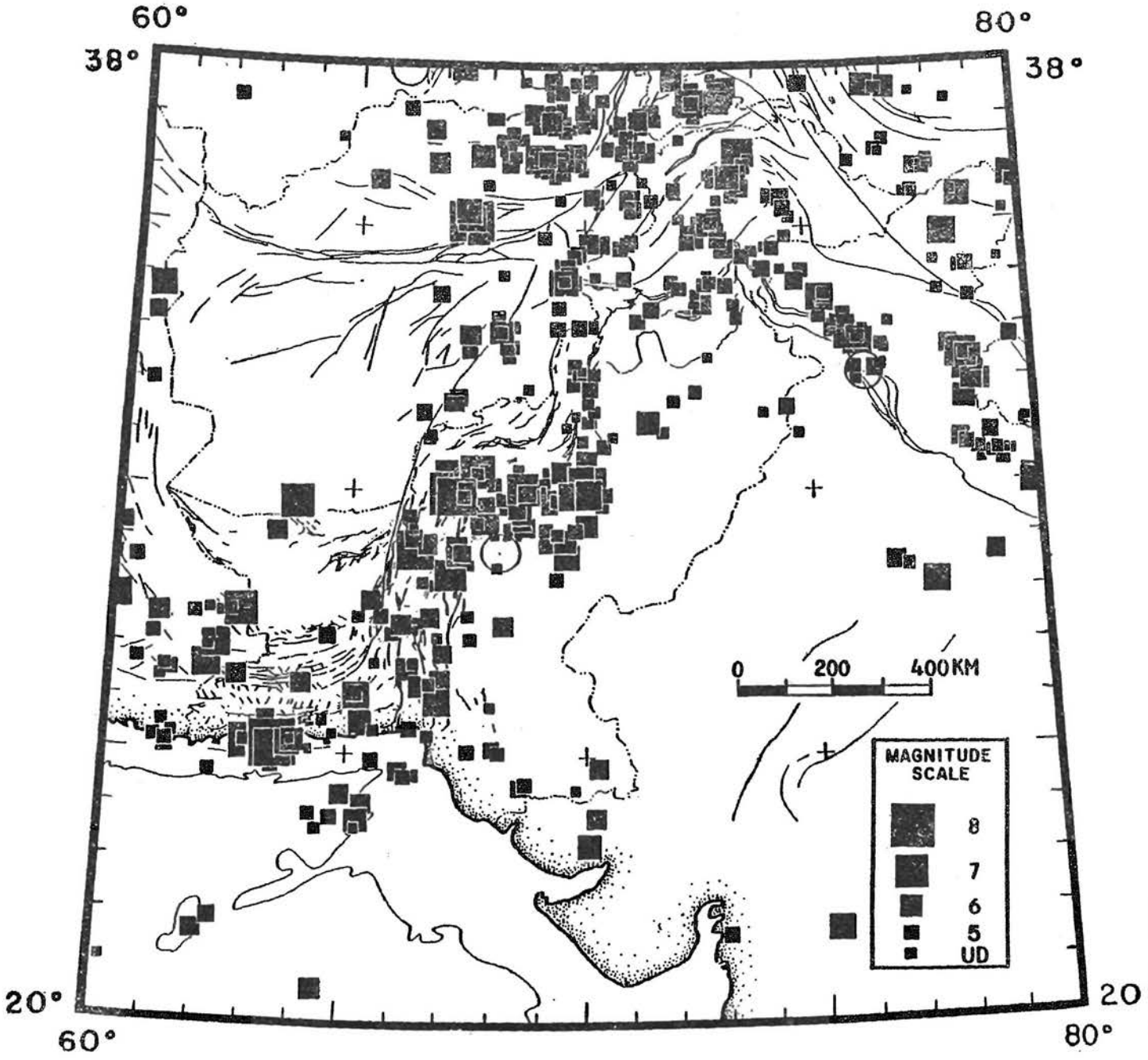

Fig. 3. Epicentral map of crustal seismicity (depth h < 85 km) for Pakistan and surrounding regions (compare with Figure 2) from 1914 to 1975. Events from 1914 to 1964 have been relocated. Open circles represent large earthquakes that occurred from 1905 to 1914. UD = Undetermined magnitude. Open circles, events 1905-1914. (From Quittmeyer and Jacob, 1979).

zone of the 1909 event, the aftershock zone of the 1931 event and the ongoing seismic activity of the Quetta transverse ranges (Quittmeyer *et al.*, 1979) attest to the complexity of the active tectonic patterns of this area.

Within the area in which earthquakes were located by the Quetta seismic network there have been three historic earthquakes with an intensity (Modified Mercalli scale) of eight and greater. In addition a number of earthquakes which occurred prior to installation of the Quetta seismic network were large enough to be located by seismic instruments operating around the world (teleseismic epicenters; Figures 3 and 4).

The *20 December 1892* event brought attention

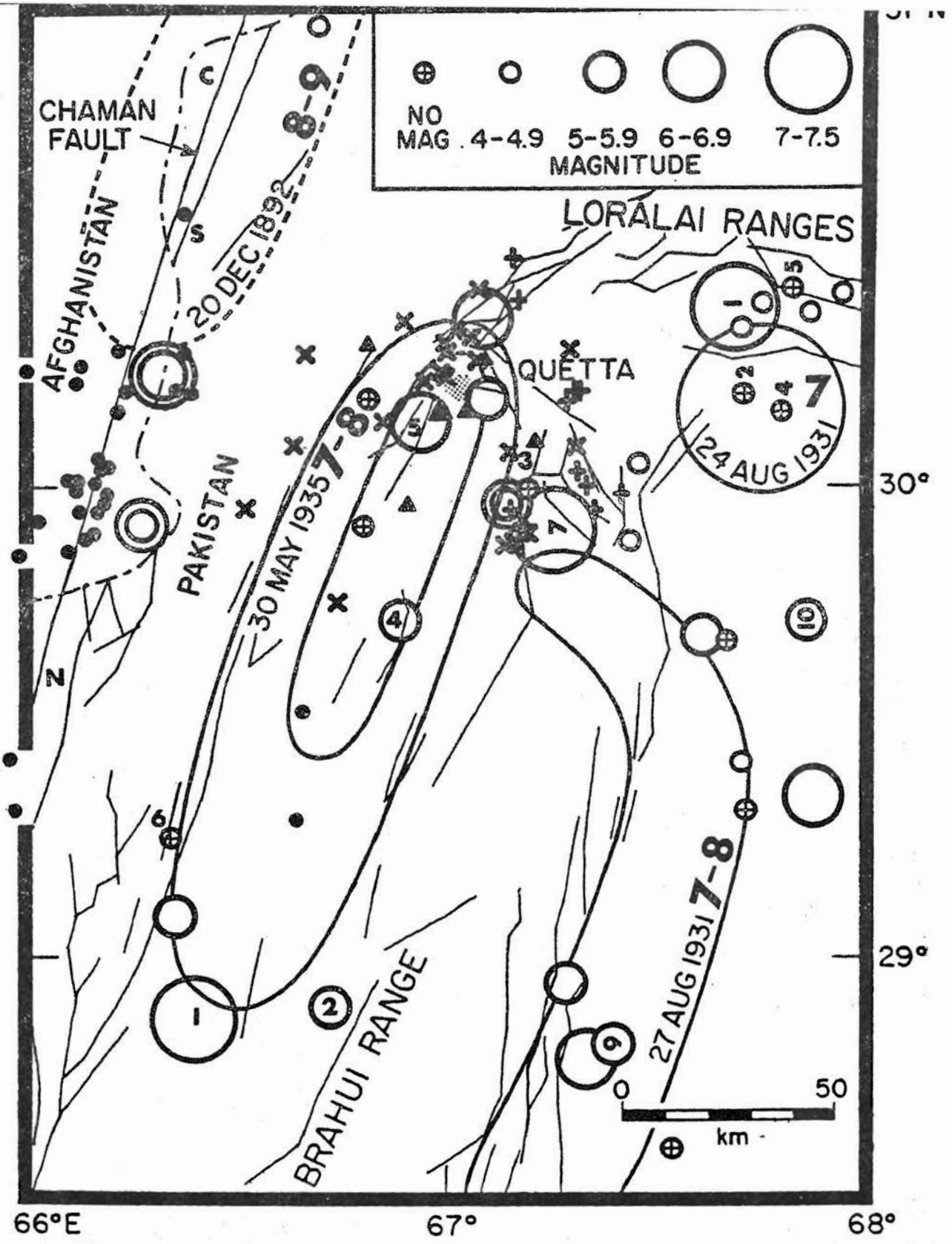

Fig. 4. Earthquake epicenters in the Quetta area from 1914 to July 1975 (open circles) and Modified Mercalli isoseismals for the three largest earthquakes in this period as well as the 1892 event (from Quittmeyer and Jacob, 1979). Double circles indicate epicenters for earthquakes occurring after this time period: The 3 October 1975, magnitude Ms = 6.7, 6 4, Spin Tezha earthquakes; the 13 July 1977, magnitude Ms = 5.5, Kolpur earthquake southeast of Quetta; and the 16 March 1978, magnitude Ms = 5.9, Nushki earthquake. C = town of Chaman; S = Spin Tezha; N = Nushki. Sequences of events are indicated by number: 1935 Quetta = numbers upright, 1931 Mach = numbers facing right (some fall outside the map). Preliminary epicenters from the Quetta network (filled triangles) are indicated by X (hypocentral depth ranges from 0 to 15 km), + (hypocentral depth ranges from 15 to 30 km), and filled circles (hypocentral depth fixed at 15 km). Note the recent (1975) increase of seismicity on the section of the Chaman fault in this figure and the striking relation between the 1892 mezoseismal area and the recent seismicity on this fault.

crust. A left-lateral strike-slip movement was observed where a railway line crosses the fault (at approximately 30.85°N, 66.52°E; Griesbach, 1893). Elders from villages along the trace of the fault in this area indicated that previous events had produced surface faulting three times during their lifetimes (McMahon, 1897).

Two teleseismic locations in the area of Figure 4 can be associated with the Chaman fault. A focal mechanism solution for the 3 October 1975 (magnitude M_s = 6.4) event (Quittmeyer et al., 1979) gives left-lateral strike-slip on a steeply dipping plane of the expected strike for the Chaman fault. Farah (1976) reported ground cracks in alluvium associated with this event along the Chaman fault-trace in Pakistan near the town of Spin Tezha, north of the epicenter in Figure 4. Observed motion was left-lateral as well as west side up with amplitudes of a few centimeters. First-motion data for the 16 March 1978, Nushki event (magnitude M_s = 5.9) is consistant with left-lateral strike-slip on the Chaman fault, but conclusive data is not yet available from this earthquake.

The *24/27 August 1931* earthquakes, M = 7.0 and M = 7.4, respectively, and the related aftershocks are associated with a complex system of faults near the axis of the syntaxis. The mezoseismal zone of the August 27 event is extended south-southwest along the eastern flank of the Brahui range (Figure 4). However, all except one of the aftershocks of this event (Quittmeyer and Jacob, 1979) lie outside of the mezoseismal zone and form a northwest trending pattern parallel to and north of the 1909 mezoseismal area (Figure 2). The instrumental epicenter of the mainshock is at the intersection of these two zones (at 29.9N and 67.3E in Figure 3). At least two faults are probably involved in the August 27 event, one striking northwest along the aftershock zone, another south-southwest along the mezoseismal zone. The very little information available about the August 24 event indicates that the ruptures associated with this earthquake are not contiguous with the August 27 rupture.

The city of Quetta was almost totally destroyed by the *30 May 1935* earthquake with loss of life in excess of 30,000 persons. The maximum intensities were observed from Quetta south-southwestward to Mastung (Figure 5) and Kalat (29.0°N, 66.6°E) thus defining a narrow and approximately linear mezoseismal zone about 150 km long (West, 1935). The epicentral location of the main shock near Kalat and aftershocks near Quetta fall in the same zone (Figure 4). On the east face of Chiltan, the prominent mountain ridge west of Quetta (Figure 5), unusually numerous rock falls were observed. A sequence of cracks in the alluvium aligned with these rockfalls was followed to the south-southwest of Chiltan. Along this line of fissures a railroad was most severely disrupted ("R" in Figure 5). The sense of motion was not reported but the description of the ground cracks indicates little vertical displacement and a predominant strike-slip motion. The pattern of destruction in Quetta indicates a maximum acceleration in the north-south direction and is consistent with the near-field effects from strike-slip on a fault that coincides with the mezoseismal zone (Figure 4).

In conclusion, the intensity data suggest that the fault responsible for the 1935 Quetta earthquake outcrops along the east face of Chiltan and extends to the south-southwest (Jones, 1961, p. 373). The northern extent of rupture along this fault probably coincides with the northern end of the Chiltan ridge (Figure 5) as indicated by the rapid fall-off of intensity north of Quetta and by the aftershock distribution. The narrowness of the zone of highest intensity suggests a shallow depth of rupture.

The Chiltan fault along the eastern flank of the Chiltan ridge is one of a set of westward-dipping parallel faults that occur in the northern portion of the mezoseismal zone (Figures 4 and 6). However, a direct correlation between these faults and the 1935 rupture is not obvious as no displacement was reported along any of these surface traces at the time of the earthquake. Thus, the fault associated with the 30 May 1935 Quetta earthquake is here refered to as the "Quetta fault".

On 18 February 1955 an earthquake (magnitude 6.2) occurred near the northern end of the Quetta earthquake rupture (Figures 4 and 7). Kazmi (1979) reports one kilometer length of ground fracture northwest of Quetta on an extension of the Chiltan fault beneath alluvium. This event may have extended the 1935 rupture northward.

MICROSEISMIC DATA

Locations for 62 small earthquakes (Figures 4 and 5) are obtained from the analysis of two months of data from the Quetta seismic network (October and November, 1978, a period during which all seismic stations operated reliably). In this preliminary study, the crustal structure determined for the Tarbela area in the Hazara arc of northern Pakistan (Armbruster *et al.*, 1978) was used for computing hypocenters by a modified form of the program "HYPO 71" (Lee and Lahr, 1972). In a first approximation, it is reasonable to assume a similar velocity structure in the Hazara arc and in the Sibi re-entrant, since both are sections of the thrust and fold belt that stretches along the northwestern boundary of the Indian craton. Accurate hypocentral depths could be determined for earthquakes less than 40 km from the nearest seismic station. Beyond this distance from the network, less reliable

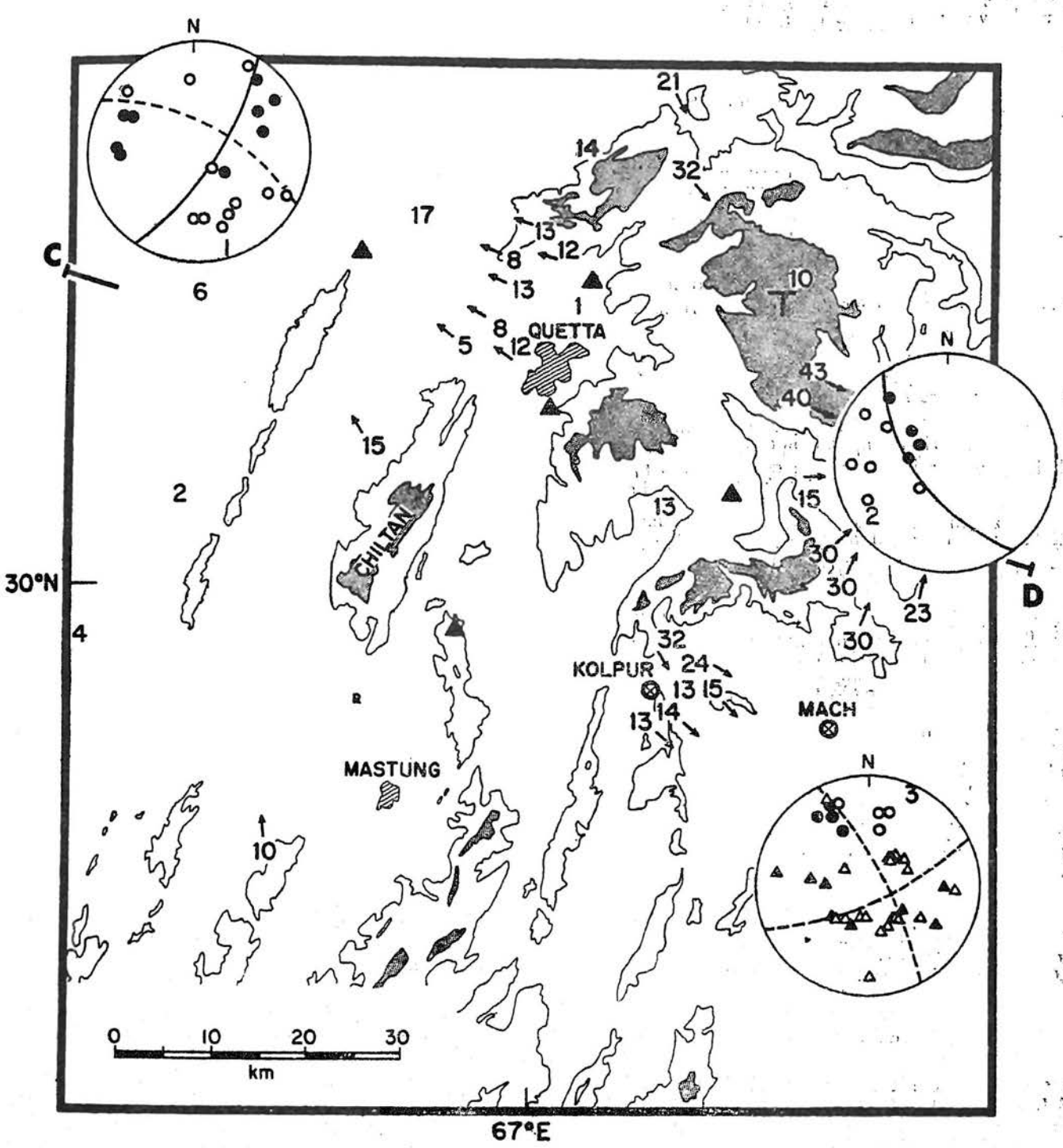

Fig. 5. Detailed map of the local activity recorded by the Quetta seismic network (triangles). Events are indicated by a number which gives hypocentral depth in kilometers. Topographic contours at 2000 and 2500 meters are shown with areas above 2500 m shaded. "T" indicates Oligocene to Pleistocene age deposits which have been uplifted. Three composite focal mechanism solutions are shown in upper hemisphere projections; filled circles compressions open circles dilitations. Arrows indicate events which were included in each composite. The number identifying the fault plane solution lies at the position of the axis of maximum compression ("2" is at the position consistent with thrusting). Solution number 3 also includes teleseismic data (triangles) for a large event which occurred before the network began operating (July 13, 1977; see Figure 4). Some geographic features referred to in the text are indicated. Section C-D is shown in Figure 6.

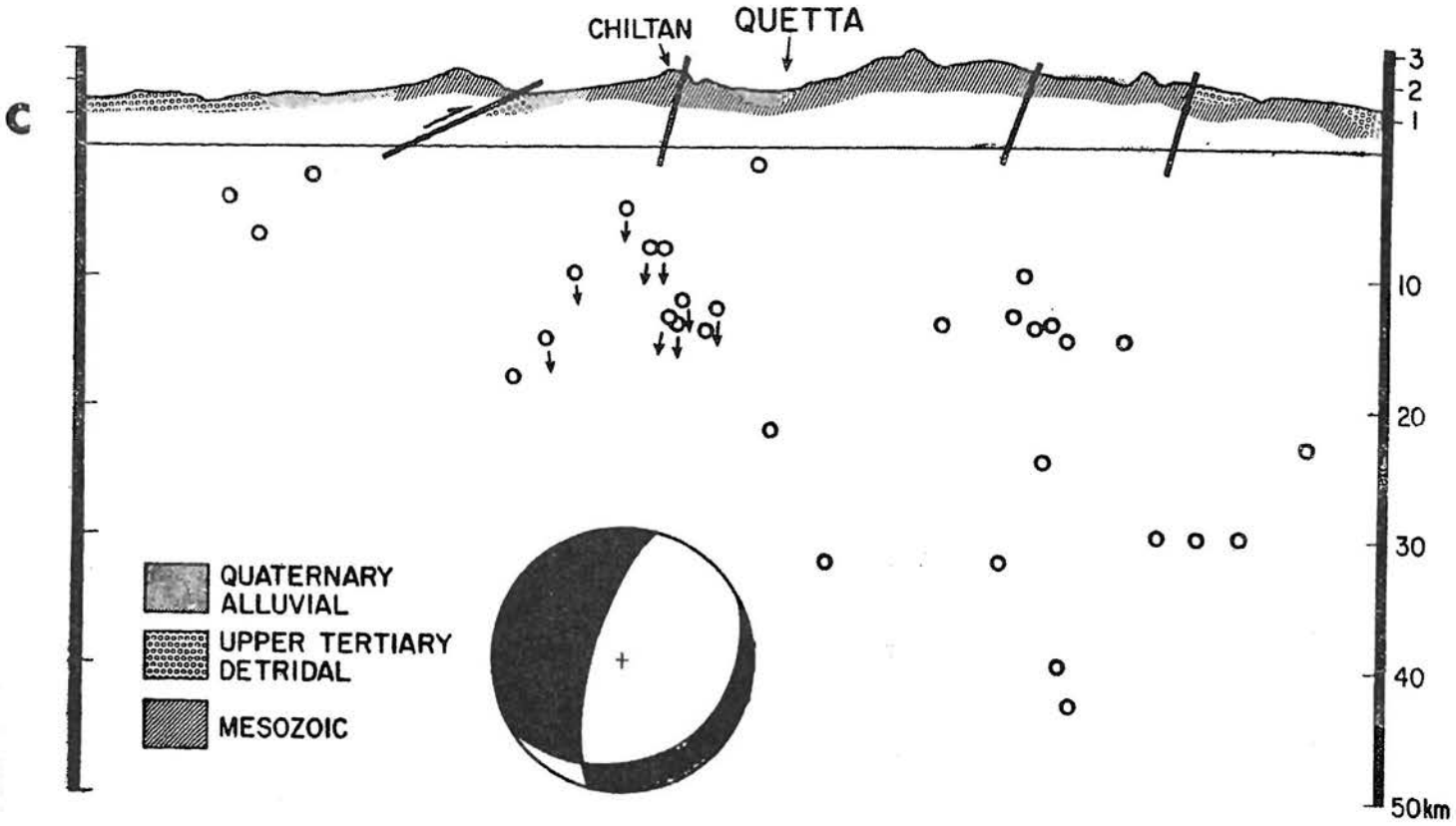

Fig. 6. Vertical cross section (C-D in Figure 5) through the Quetta seismic network with main geologic structures (Jones, 1961). Note that Upper Tertiary includes the Pleistocene in many cases. Small circles indicate hypocenters determined by the Quetta seismic network. The focal mechanism for events along the fault which is presumed to have ruptured in the 1935 Quetta earthquake is also shown (upper hemisphere, viewed from this side, compressional quadrant shaded). Note the agreement between the Chiltan fault on the east face of Chiltan, and the fault plane as determined by the focal mechanism. Some of the scatter in the seismicity related to this mechanism can be attributed to bending of the fault trace north of the Quetta valley. The shallow dipping fault to the west also appears to be active. The activity in the eastern half of the figure is not oriented well for viewing in this projection.

epicenters were obtained arbitrarily fixing the depth at 15 km. In the latter category are all the epicenters obtained in the Chaman fault area.

Chaman Fault: This fault is the most active seismic zone observed by the Quetta network. About half of all the microearthquake epicenters in Figure 4 occur along the Chaman fault, within the possible error in location. Considering the distance of this fracture from the network (~ 70 km), this seismic source must be at least an order of magnitude more active than the area within the seismic network. Most of these microearthquakes fall on the same segment of the Chaman fault presumably associated with the two recent teleseismically located events, the 3 October 1975, magnitude M_s 6.4 and 6.7 Spin Tezha earthquakes, and the 16 March 1978, magnitude M_s 5.9 Nushki earthquake (Figure 3). It is possible that the microearthquakes occurring on the Chaman fault 36 and 7 months, respectively, after these moderate size earthquakes are part of a prolonged and complex aftershock sequence.

Quetta Fault: The northern portion of this fault, which by definition ruptured in the 1935 Quetta earthquake, is well covered by the Quetta network. A number of hypocenters aligned with the Chiltan ridge and located northwest of Quetta are probably associated with this fault (Figure 5). Most of these hypocenters cluster near the northern end of the 1935 mezoseismal zone and occur to the north of all the located 1935 aftershocks (Figure 4). It is possible that most of the current seismicity on the Quetta fault occurs beyond but near the north end of the 1935 rupture (Figure 7). Only four epicenters correlate with the central portion of the fault which ruptured in 1935.

The hypocentral locations, focal mechanism and mapped faults (Jones, 1961) are all consistent with a

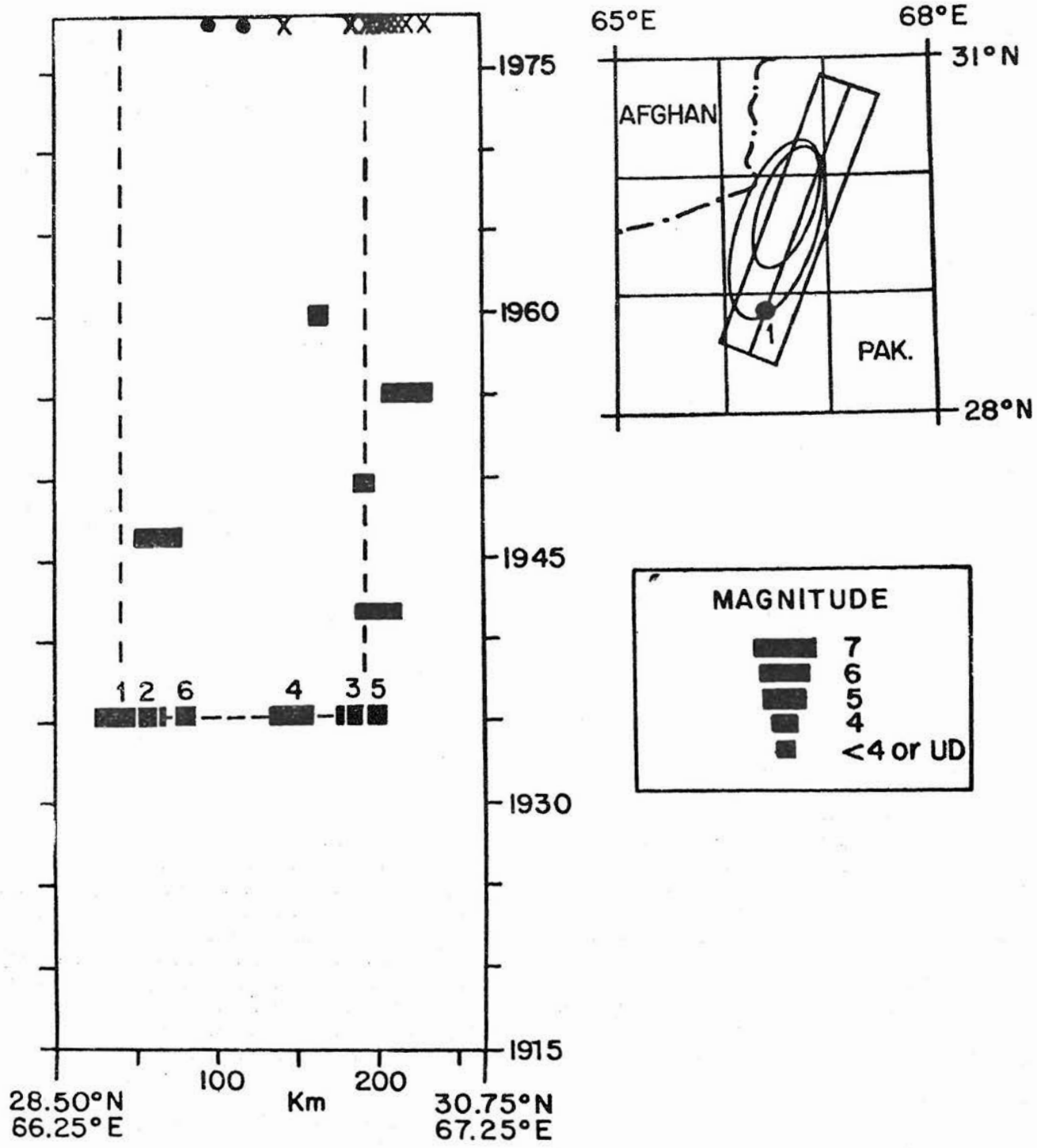

Fig. 7. Space-time for the Quetta fault. In the map, the box gives the area sampled; the isoseismals and the epicenter for the 1935 earthquake are shown for reference (see Figure 4). The dashed lines indicate the extent of the aftershock zone. Crosses and dots in 1978 are the epicenters from the network data (see Figure 4). Note that the seismicity after the 1935 earthquake is concentrated near the ends of the rupture associated with this earthquake.

fault or fault-zone striking north-northeast and steeply dipping to the west-northwest. The apparently complex distribution of hypocenters on the Quetta fault-zone in Figure 6 may be ascribed to activity on more than one parallel faults and/or to the bending of these faults north of the Quetta valley. The composite focal mechanism of these events (Figures 5 and 6) indicates the northern portion of the Quetta fault is presently strike-slipping in a left-lateral sense.

Other Active Zones: Three shallow hypocenters occur west of the network but within the area of Figures 5 and 6. These events fit well with the shallow-dipping thrust-fault associated with the next ridge west of Chiltan along this fault. Mesozoic limestone is thrusted eastward over Pleistocene sediments, further suggesting that this is a recent fault (Jones, 1961; Gansser, 1979).

In general, the maximum hypocentral depth increases eastward across the network (Figure 6). The deepest hypocenters at 43 km occured east of Quetta below Zarghun mountain at the axis of the Sibi re-entrant. The first motion data for the earthquakes in this area deeper than 15 km (Figure 5, Solution # 2) define a north westward striking plane which is consistent with the spatial distribution of the hypocenters, and, in the context of this limited data, can be taken as the plane of rupture. According to the first-motion data this plane dips steeply to the northeast and the motion could range from pure dip-slip, north side up, to pure left-lateral strike-slip. A reverse slip on this fault is consistent with the recent and probably ongoing uplift of the Zarghun range where Pleistocene molasse of the Urak group (Jones, 1961, p. 312-314) is more than 3.5 km above sea level (T in Figure 5). Left lateral strike-slip is consistent with the surface displacement on the Mach fault (Kazmi, 1979), the trace of which is directly up-dip from this seismic structure. An oblique slip would account for both surface features. Seeber and Armbruster (1979) have argued that a detachment probably decouples the surface structures surrounding the Sibi re-entrant from the basement. Note that focal mechanism solutions (Figure 5) include events either all greater than or all less than approximately 15 km deep. If a detachment decouples the upper 15 kilometers of the crust from the lower crust, the correlation between the Mach fault and the seismic structure of fault-plane solution 2 in the deep crust (Figure 5) is fortuitous.

The moderate (Ms = 5.5) earthquake of 13 July 1977 was most strongly felt in Kolpur (Figure 5) and was teleseismically located near there (Figure 4). A tight cluster of hypocenters from the network data occur quite close to the teleseismic epicenter of the Kolpur event. Solution # 3 of Figure 5 contains first-motion data of both the microearthquakes and the larger event. The teleseismic data (first motion reported in bulletins only) obviously contains a number of inconsistent points. The composite data are equally compatible with normal faulting and strike-slip faulting, both with an east-west tension axis. The strike slip solution is more compatible with the general tectonic environment of the study area and with the hypocentral depth of the microearthquakes in the lower crust where normal faulting usually is not observed.

In the strike slip solution shown in Figure 5, the northeast striking plane with left-lateral slip coincides with the north westward alignment of the microearthquake data. However, the epicenter of the 27 August 1931 Mach earthquake is also close to Kolpur (29.91°N, 67.25°E, Figure 4). The northwest trend of the aftershock pattern of that event indicates that a major northwest striking fault, perhaps in the lower crust, is active in the Kolpur area. The northwest striking plane with right-lateral slip in solution No. 3 (Figure 5) could be associated with such a fault.

CHAMAN FAULT VS. SAN ANDREAS FAULT

Historic, teleseismic and network data examined together indicate that since 1975 the pattern of seismicity in the Quetta area is characterized by unusually high activity on the Chaman fault west of Quetta.

A 3/4 meter displacement was observed on the Chaman fault near the town of Chaman after the 1892 event (Griesbach 1893). In contrast to reports indicating repeated offsets on the Chaman fault occurring in the 19th century (McMahon, 1897), no offsets are reported for the period between 1892 and 1975 (Figure 2) although two railways cross the fault (at 30.8°N and 29.4°N) and the area has been occupied by military garrisons.

A pattern similar to the distribution of reported intensities (Figure 2) is obtained from the teleseismic data prior to 1975 (Figure 3). The seismicity along the fold belt east and south of Quetta is generally high, but no epicenters occur along the Chaman fault south of latitude 31°N. However, most of the seismicity detected since 1975 in the area of Figure 4 is concentrated along the Chaman fault south of the southern limit of the 1892 mezoseismal area at about 30.3°N (Heuckroth and Karim, 1970). This recent seismicity includes two teleseismic epicenters, the Spin Tezha 1975 (Ms = 6.4 and 6.7) and the Nushki 1975 (Ms = 5.9) earthquakes, and most of the microearthquakes detected by the Quetta network.

Thus, there has been a recent increase of seismicity on the Chaman fault south of the 1892 event. However, the possibility of another such burst of activity on this section of the Chaman fault after 1892 and before 1963, when the teleseismic detection level in this area was lowered to about magnitude Mb = 4.8 (Seeber *et al.* 1979), cannot be ruled out.

The seismicity along the Quetta fault after the 1935 event is also concentrated at the extremities of the fracture zone as determined from the mezoseismal area. Four out of five of the teleseismic epicenters that can be related with the Quetta fault occur within 30 km of either of the extremities of the 150 km long presumed rupture (Figures 4 and 7). Given the uncertainty of the locations these earthquakes may have occurred on the Quetta fault very near the extremities of the fracture. The February 18, 1955 (M 6.2) event is particularly significant because a mile-long fissure was observed after this event along the northern extension of the Chiltan fault in the Quetta valley north of Quetta, at the presumed northern extremity of the 1935 rupture. The network data for the Quetta fault (Figures 4 and 5) confirm the pattern of seismicity indicated by the teleseismic data. Microearthquake hypocenters cluster in a 30 km segment of the Quetta fault at the northern extremity of the 1935 rupture.

Thus, the general pattern of seismicity in the Quetta area is one of large events and aftershock sequences. During the interseismic periods the segments of the faults that ruptured at the large events are almost aseismic and the seismicity is concentrated at the extremities of these segments. Such a pattern has been observed in California along the San Andreas fault system (Allen, 1975). The 150 km long segment of the San Andreas fault between the northern end of the 1857 and the southern end of the 1906 breaks never ruptured in a major event during historic times. A detailed examination of surface displacement and geodetic data in this segments of the fault (Brown and Wallace, 1968; Savage and Burford, 1973) indicate that the slip in the last 60 years has been rather continuous and uniform at about 3.2 cm/year, a rate which probably corresponds to the long term rate of slip. Thus, strain energy for a large event in this segment of the San Andreas fault is not accumulating. In the same segment, the seismicity is characterized by small and intermediate earthquakes ($M < 6.5$; see below) with relatively short recurrence times (an earthquake which is "intermediate" may still be destructive locally). On the other hand, in the segment of the San Andreas fault that ruptured in 1857, major earthquakes have occurred systematically over the past 14 centuries at an average rate of 1 earthquake every 160 years (Sieh, 1978) but few small earthquakes are occurring there now. Thus, the San Andreas fault is characterized by distinct portions with contrasting and stable patterns of behaviour.

The San Andreas fault system in California and the Alpine fault system in New Zealand exhibit change in strike or bends such that the angle between the regional slip-vector and the strike of the master-fault varies along the fault system. Scholz (1977) compares the portion of the San Andreas fault that ruptured in 1857, known as the "big bend", with the central portion of the Alpine fault of New Zealand adjacent to the southern Alps (Figure 8). This section of the Alpine fault has not ruptured in historic time (150 years), it is not associated with intermediate or small earthquakes, it is not creeping, and it is expected to rupture in a major event, similar to the 1857 event. (Following Scholz, the magnitude in a major earthque is $M > 7.5$, in a large earthquake $7.5 \geq M \geq 6.5$, in a moderate or small earthquake $M < 6.5$; with this definition the Quetta 1935 $M = 7.5$, is classified as a large but not major earthquake).

It is here suggested that the segment of the Chaman fault between 30°N and 33°N that includes the 1892 rupture (only the southern limit of this rupture is approximately known) fits in the same category as the segments of the San Andreas and Alpine faults mentioned above, i.e., strain relief by rare but major events.

In all these three segments the fault zone is rather narrow and it may rupture only in major earthquakes. Scholz ascribes this behaviour to the relatively large angle between the slip-vector and the strike of the fault which would, in all three cases, tend to increase the normal component of stress across the fault, and hence the frictional strength. In each of the regions in Figure 8, south of the "bend" the strike of the fault system is nearly parallel to the regional slip. In these areas the fault zone widens and slip appears to be taken up by a number of subparallel faults. Furthermore, in these same sections of the fault-zones major earthquakes do not occur, but large to small earthquakes occur frequently and, together with possible creep-zones, probably account for the total long-term slip-rate across the fault-zones (see Figure 3). Data presented in this paper indicate that the Quetta 1935 event ruptured a fault subparallel to the Chaman fault and accounted for a portion of the left-lateral strike-slip taken up by this fault system.

Lawrence and Yeats (1979) have investigated the portions of the Chaman fault in Pakistan. They contrast the "long, straight active trace" of the fault in the area of the 1892 event with the "short traces, multiple *en echelon* traces and local absence of active traces" observed to the south, in the Nushki area. From a comparison of the contrasting surface features along the 1906 break and the "creeping" segmtnt of the San Andreas fault with the similarly contrasting features along the 1892 segment and the Nushki segment of the Chaman fault, they suggest a pattern of major earthquakes versus creep and small earthquakes in these two segments of the Chaman fault, respectively.

The surface-wave to body-wave magnitude ratio, M_s/M_b, for the three recent earthquakes in the area of

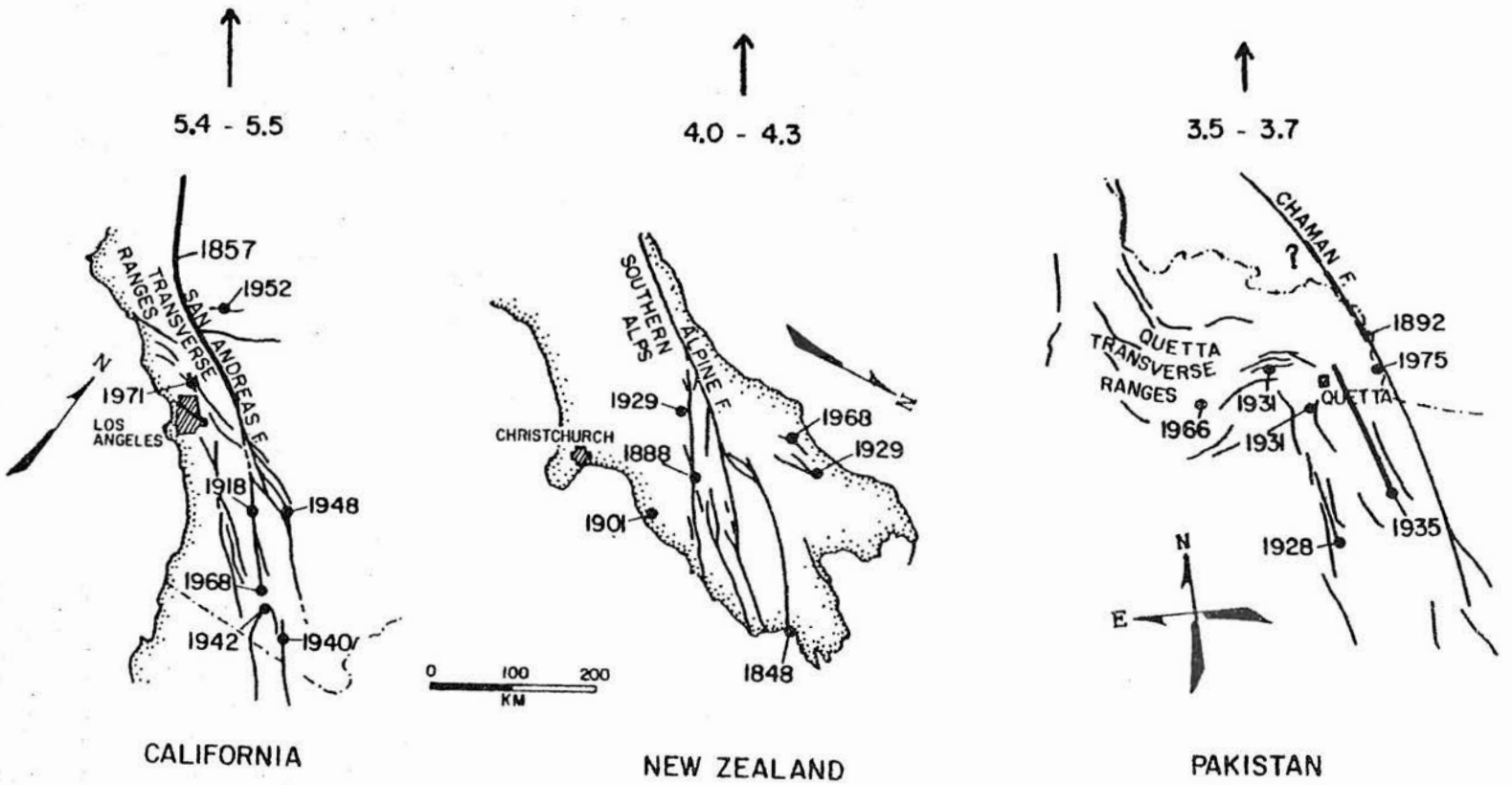

Fig. 8. Fault maps of southern California and South Island New Zealand (from Scholz, 1977) and the Quetta area, Pakistan. They have been rotated so that the regional slip vectors (arrows above) are parallel and Pakistan has east and west reversed to give right-lateral strike-slip in all three areas. Length of the slip vector is proportional to the approximate rate of relative motion between major plates (rate given in cm/yr). Dates of earthquakes and zones of rupture mentioned in the text are indicated.

Figure 4, the Spin Tezha 1975, the Nushki, 1978, and the Kolpur 1977 events, are 6.4/5.7, 6.7/5.8, 5.9/5.3, and 5.5/5.1, respectively (Epicenter Determination Report, U.S.G.S.). The unusually high ratios for the three earthquakes on the Chaman fault suggest low stress-drops for these earthquakes (Archambeau, 1978). Similarly the stress-drops for earthquakes along the San Andreas fault are low and generally lower than for other earthquakes in Southern California (Thatcher and Hanks, 1973). Since the recent instrumental seismicity associated with both the San Andreas and the Chaman faults occur along segments of these faults between major ruptures, the low stress-drops may characterize these segments only, and not necessarily the rest of the fault where major earthquakes occur.

CONCLUSIONS

1. The Chaman fault and the Quetta fault (which ruptured in the 30 May 1935 earthquake) exhibit left-lateral strike-slip motion.

2. The seismicity deepens to the east across the Quetta network: it is confined in the upper 20 km along the Quetta fault zone but reaches deeper than 40 km below the Zarghun Range, 30 km east of Quetta. This seismicity may be related to a dual level tectonics similar to that observed in the Hazara arc region near Tarbela dam.

3. On the Chaman fault and Quetta fault, small to intermediate earthquakes are concentrated at the ends of zones which ruptured in large or major earthquakes.

4. The Chaman fault and the San Andreas fault are both considered transform faults at plate boundaries. The spatial and temporal distribution of seismicity of major, intermediate and small earthquakes, the stress-drop character and surface morphology of the fault trace appears to be similar in both these faults.

5. A seismically quiescent period along the Chaman fault south of 30.3°N and north of Nushki (at least for magnitudes $M \geq 4.8$) has ended in 1975. Since then, in this 60 km long segment of the fault, three moderate (Ms = 6.7, 6.4, 5.9) and many small earthquakes have occurred. This recent change in the seismic pattern may be a premonitory signal.

Acknowledgements: This project would not have been possible without the support of the Geological Survey of Pakistan and its personnel in establishing and maintaining the instruments in the field. K. DeJong was instrumental in the organizational aspects The Water and Power Development Authority loaned the project some essential equipment. Klaus Jacob and Terry Engelder reviewed the manuscript. This work was supported by the following grants: USGS 14—08—0001—16749; NSF Internaitonal, INT 76—22304 (Univ. of Cincinnati, K. DeJong); and NSF EAR 77—15187)

REFERENCES

Allen, C.R. (1975). Geological criteria for evaluating seismicity, *Geol. Soc. Amer. Bull.*, 86, 1041—1057.

Archambeau, L. (1978). Estimation of non-hydrostatic stress in the earth by seismic methods: Lithospheric stress levels along Pacific and Nazca plate subduction zones, Proceedings of Conference VI Methodology for identifying seismic gaps and soon to break gaps, U.S.G.S. Open-File Report 78—943.

Armbruster, J., L. Seeber, and K. H. Jacob (1978). The northwestern termination of the Himalayan mountain front. Active tectonics from microearthquakes, *J. Geophys. Res.*, 83, n. Bl, 269—282.

Brown, R.D., and R E. Wallace (1968). Current and historic fault movement along the San Andreas fault between Paicines and Camp Dix, California, Proceedings of the Conference on Geologic Problems of the San Andreas Fault System, *Stanford Univ. Publ. Univ. Ser. Geol. Sci.*, 11, 22—41.

Farah, A. (1976). Study of recent seismotectonics in Pakistan: Report CENTO Working Group on Recent Tectonics, Istanbul.

Gansser, A. (1979). Reconnaissance visit to the ophiolites in Baluchistan and the Himalayas, In: *Geodynamics of Pakistan,* A. Farah and K. DeJong (eds.).

Griesbach, C.L. (1893). Notes on the earthquake in Baluchistan on the 20th December 1892, *Rec. Geol. Sur. India,* 26, n. 1, 47—61.

Heron, A M. (1911). The Baluchistan earthquake of the 21st October 1909, *Rec. Geol. Sur. India,* 41, part 1, 22—35.

Heuckroth, L.E., and R.A. Karim (1970) *Earthquake history, seismicity, and tectonics of the regions of Afghanistan,* Kabul University, 102 p.

Jones, A.G. (ed.) (1961). Reconnaissance geology of part of West Pakistan; A Colombo Plan Cooperative Project, Government of Canada, Toronto, 550 p.

Kazmi, A.H. (1979). Active fault systems in Pakistan, in *Geodynamics of Pakistan,* A. Farah and K. DeJong (eds.), Spec. Publ. GSP, Quetta.

Lawrence, R.D., and R.S. Yeats (1979). Geological reconnaissance of the Chaman fault in Pakistan, in: *Geodynamics of Pakistan,* A. Farah and K. DeJong (eds.), Spec. Publ. GSP, Quetta.

Lee, W.H.K, and J.C. Lahr (1972). HYPO 71 (revised): A computer program for determining hypocenter, magnitude, and first motion pattern of local earthquakes, U.S.G.S. Open-File Report 75-311.

McMahon, A.H. (1897). The southern borderlands of Afghanistan, *The Geographical Jour.,* 9, n. 4, 393-415.

Middlemiss, C.S. (1910). The Kangra earthquake of 4th April 1905, *Mem. Geol. Sur. India,* 38, 1-409.

Minster, J.B., and T.H. Jordan (1978). Present-day plate motions, *J. Geophys. Res.,* 83, 5331.

Molnar, P., and P. Tapponnier (1975). Cenozoic tectonics of Asia: Effects of a continental collision, *Science,* 189, 419-426.

Powell, C.McA. (1979). A spectulative tectonic history of Pakistan, in: *Geodynamics of Pakistan,* A. Farah and K. DeJong (eds.), Spec. Publ. GSP, Quetta.

Quittmeyer, R C., and K.H. Jacob (1979). Historical and modern seismicity in Pakistan, Afghanistan, Northwest India, and Southeast Iran, *Bull. Seism. Soc. Am.,* 69, 773-823.

Quittmeyer, R.C., A. Farah, and K H. Jacob (1979). The seismicity of Pakistan and its relation to surface faults, in: *Geodynamics of Pakistan,* A. Farah and K. DeJong (eds.), Quetta, p. 271-284.

Savage, J C., and R.O. Burford (1973). Geodetic determination of relative plate motions in Central California, *J. Geophys. Res.,* 78, 832-845.

Scholz, C.H. (1977). Transform fault systems of California and New Zealand: Similarities in their tectonic and seismic styles, *J. Geol. Soc.,* 133, 215-229.

Seeber, L., and J. Armbruster (1979). Seismicity of the Hazara arc in northern Pakistan: Decollement vs. basement faulting, In: *Geodynamics of Pakistan,* A. Farah and K. DeJong (eds.), Quetta, p. 131-142.

Seeber, L., J. Armbruster, and S. Farhatulla (1979). Seismic hazard at the Tarbela dam site and surrounding region from a model of the active tectonics, preprint.

Seeber, L., R C. Quittmeyer, and J. Armbruster (1979). Himalayan earthquake belts: Implications from network data from the western syntaxial area, submitted to *Structural Geology of the Himalayas,* ed. P.S. Saklani, Delhi University.

Sieh, K.E. (1978). Prehistoric large earthquakes produced by slip on the San Andreas fault at Pallett Creek, California, *J. Geophys. Res.,* 83, 3907.

Thatcher, W., and T.C. Hanks (1973). Source parameters of southern California earthquakes, *J. Geophys. Res.,* 78, 8547-8576.

West, W.D. (1934). The Baluchistan earthquakes of August 25th and 27th, 1931, *Mem. Geol. Sur. India,* 67, part I, 1-82.

West, W.D. (1935). Preliminary geological report on the Baluchistan (Quetta) earthquake of May 31st, 1935, *Rec. Geol. Sur. India,* 69, part 2, 203-240.